Nam Nguyen

Solar Tracking System

Helsinki Metropolia University of Applied Sciences

Bachelor of Engineering

Degree Programme of Electronics

Thesis

23 May 2016

Helsinki Metropolia University of Applied Sciences

Author(s)	Nam Nguyen
Title	Solar Tracking System
Number of Pages	39 pages + 3 appendices
Date	23 May 2016
Degree	Bachelor of Engineering
Degree Programme	Electronics
Instructor	Janne Mäntykoski, Senior Lecturer

The goal of this thesis was to develop a laboratory prototype of a solar tracking system, which is able to enhance the performance of the photovoltaic modules in a solar energy system. The operating principle of the device is to keep the photovoltaic modules constantly aligned with the sunbeams, which maximises the exposure of solar panel to the Sun's radiation. As a result, more output power can be produced by the solar panel.

The work of the project included hardware design and implementation, together with software programming for the microcontroller unit of the solar tracker. The system utilised an mbed LPC1768 microcontroller to control motion of two stepper motors, which rotate solar panel in two axes. The amount of rotation was determined by the microcontroller, based on inputs retrieved from four photo sensors located next to solar panel.

At the end of the project, a functional solar tracking system was designed and implemented. It was able to keep the solar panel aligned with the sun, or any light source repetitively. A quantitative measurement was also performed, which reported how well tracking system improved output power in comparison with fixed mount.

Despite being small-scale, the project is a successful attempt in catching up with recent technologies of solar energy. Design of the solar tracker from this project is also a reference and a starting point for the development of more advanced systems in the future.

Keywords	Solar, Photovoltaic, Tracker

Contents

Appendices

Appendix 1. Circuit Diagram for TTDAT Control Board and Photo Sensor Circuit

Appendix 2. Stepper Motor Functional Module and TTDAT Software Program Code

Appendix 3. Measurement Data of Fixed Mount System and TTDAT System

List of Abbreviations

A	Ampere, SI unit of electric current
AADAT	Azimuth-altitude dual-axis tracker
AC	Alternative current
c-Si	Crystalline silicon
DAT	Dual-axis tracker
DC	Direct current
DIP	Dual in-line package
E	Dimension symbol of electromotive force
HDAT	Horizontal dual-axis tracker
HSAT	Horizontal single-axis tracker
I	Dimension symbol of electric current
LDR	Light-dependent Resistor
LED	Light-Emitting Diode
PSU	Power supply unit
PV	Photovoltaic
SAT	Single-axis tracker
TSAT	Tilted single-axis tracker
TTDAT	Tip-tilt dual-axis tracker
USB	Universal Serial Bus
V	Volt, derived unit of voltage and electromotive force
VSAT	Vertical single-axis tracker
W	Watt, derived unit of power in SI system

1 Introduction

With the unavoidable shortage of fossil fuel sources in the future, renewable types of energy have become a topic of interest for researchers, technicians, investors and decision makers all around the world. New types of energy that are getting attention include hydroelectricity, bioenergy, solar, wind and geothermal energy, tidal power and wave power. Because of their renewability, they are considered as favourable replacements for fossil fuel sources. Among those types of energy, solar photovoltaic (PV) energy is one of the most available resources. This technology has been adopted more widely for residential use nowadays, thanks to research and development activities to improve solar cells' performance and lower the cost. According to International Energy Agency (IEA), worldwide PV capacity has grown at 49% per year on average since early 2000s [1, 9]. Solar PV energy is highly expected to become a major source of power in the future.

However, despite the advantages, solar PV energy is still far from replacing traditional sources on the market. It is still a challenge to maximise power output of PV systems in areas that don't receive a large amount of solar radiation. We still need more advanced technologies from manufacturers to improve the capability of PV materials, but improvement of system design and module construction is a feasible approach to make solar PV power more efficient, thus being a reliable choice for customers. Aiming for that purpose, this project had been carried out to support the development of such promising technology.

One of the main methods of increasing efficiency is to maximise the duration of exposure to the Sun. Tracking systems help achieve this by keeping PV solar panels aligned at the appropriate angle with the sun rays at any time. The goal of this project is to build a prototype of light tracking system at smaller scale, but the design can be applied for any solar energy system in practice. It is also expected from this project a quantitative measurement of how well tracking system performs compared to system with fixed mounting method.

2 Theoretical Background

Solar energy systems, or PV systems, from compact and simple as in pocket calculators to complicated and powerful as in space station power supplies, are all made possible thanks to the phenomenon called photovoltaic effect, the conversion from solar energy to direct current electricity in certain types of semiconductors. The full understanding of the process requires understandings of different physics concepts, such as photons and solar radiation, semiconductor structure, conversion between solar radiation, chemical energy and electrical energy.

Within the scope of this project, which is developing a tracking module, the principle of the phenomenon has only been covered and explained to some extent. This part of the paper will be focusing on practical and engineering aspects of the topic, such as the structure of a PV system, its subsystems and components, mechanical setup, and other factors that influence PV systems' performance and efficiency. Especially, the structure of a solar tracking system will be covered, with some physics knowledge behind its operation.

2.1 Photovoltaic Principles

2.1.1 The Photovoltaic Effect

In semiconducting materials, the range of excitation energies is separated by an energy gap called band gap. The one below band gap (valence band) is mostly occupied with electrons of the semiconductor atoms, and the one above (conduction band) is almost empty, as described in figure 1. When electron is well excited by an amount of energy similar to the band gap, it jumps to the conduction band, creating a pair of electron-hole. In intrinsic semiconductor, the excited electron starts moving back as it loses energy (recombination). By adding other elements to semiconducting materials, extrinsic or *doped* semiconductors are created.

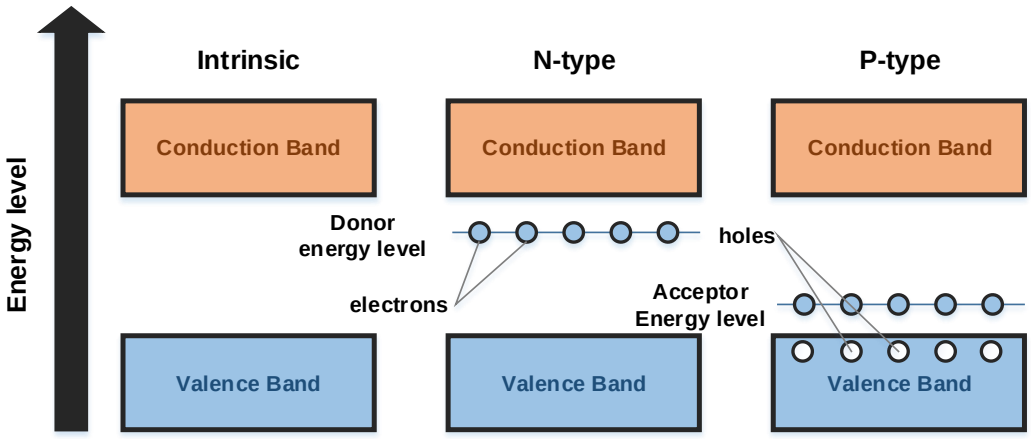

Figure 1. Excitement energy levels in intrinsic and doped semiconductor. Modified from Nipun (2015) [2]

As figure 1 also shows, n-type semiconductors contain extra amount of loose electrons from donor, and p-type semiconductors lack some electrons in their covalence bonds. This makes electron the major charge carrier in n-type and hole the major charge carrier in p-type. When connecting these two kinds of doped semiconductor, we have a P-N junction. In a P-N junction, some n-side electrons diffuse to the p-side and vice-versa for p side holes, creating a depletion region in between. This phenomenon is visually explained in figure 2 below.

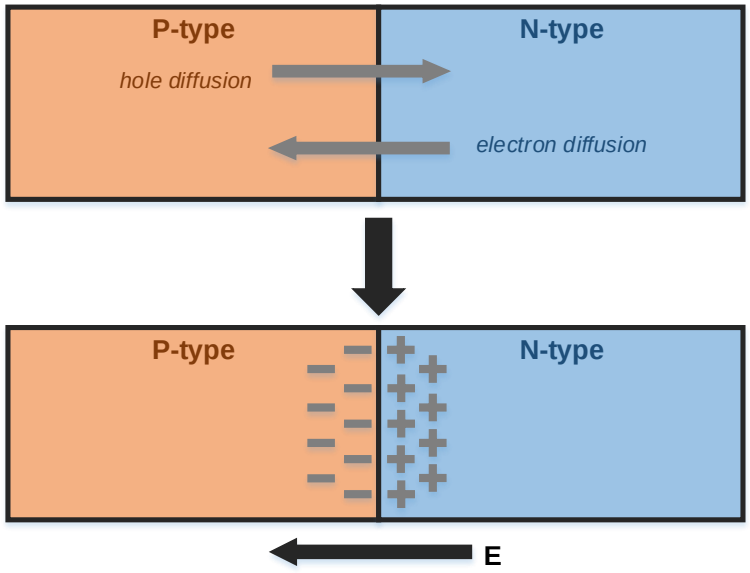

Figure 2. Depletion region and electric field E created by diffusions of electrons and holes in P-N junction. Modified from Wikimedia (2016) [3].

The depletion region in figure 2 contains positive charged part of n-type and negative charged part of p-type semiconductors. This creates an electric field that prevents further diffusion of electrons and holes, reaching an equilibrium. When exposed to the sunlight, pairs of electron-hole are created in the depletion region, and that electric field sweeps electrons and holes to N-side and P-side, respectively. Connecting an external circuit allows electrons (from n-side) to travel through and recombine with holes at the other end (p-side). This process produces an electric current that drive the load, as shown in figure 3.

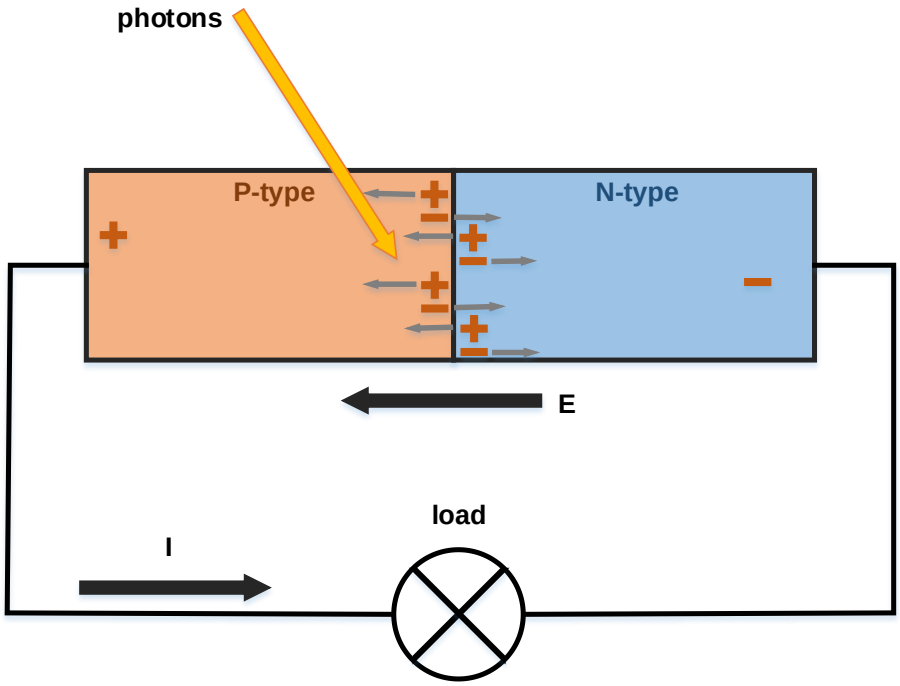

Figure 3. Occurrence of electric current I when an external circuit was connected to a P-N junction. Modified from Apec (2007) [4].

The effect explained in figure 3 is called the *photovoltaic effect*. Photovoltaic effect is the foundation for photovoltaic technology, that exploits the solar power using semiconducting materials.

2.1.2 Photovoltaic Materials and Solar Cell

Popular PV materials showed in figure 4, such as Silicon (Si), Indium phosphide (InP), Gallium arsenide (GaAs), Cadmium telluride (CdTe) or Cadmium selenide (CdSe), have spectral sensitivities match to the wavelengths of the solar radiation spectrum, since they

have band gaps correspond to lights of those wavelengths. They are the most suitable to manufacture solar cells, the building blocks of any solar PV systems. By applying different materials in multi-junction cell, wider range of solar spectrum can be absorbed, which increases the efficiency of the solar cell.

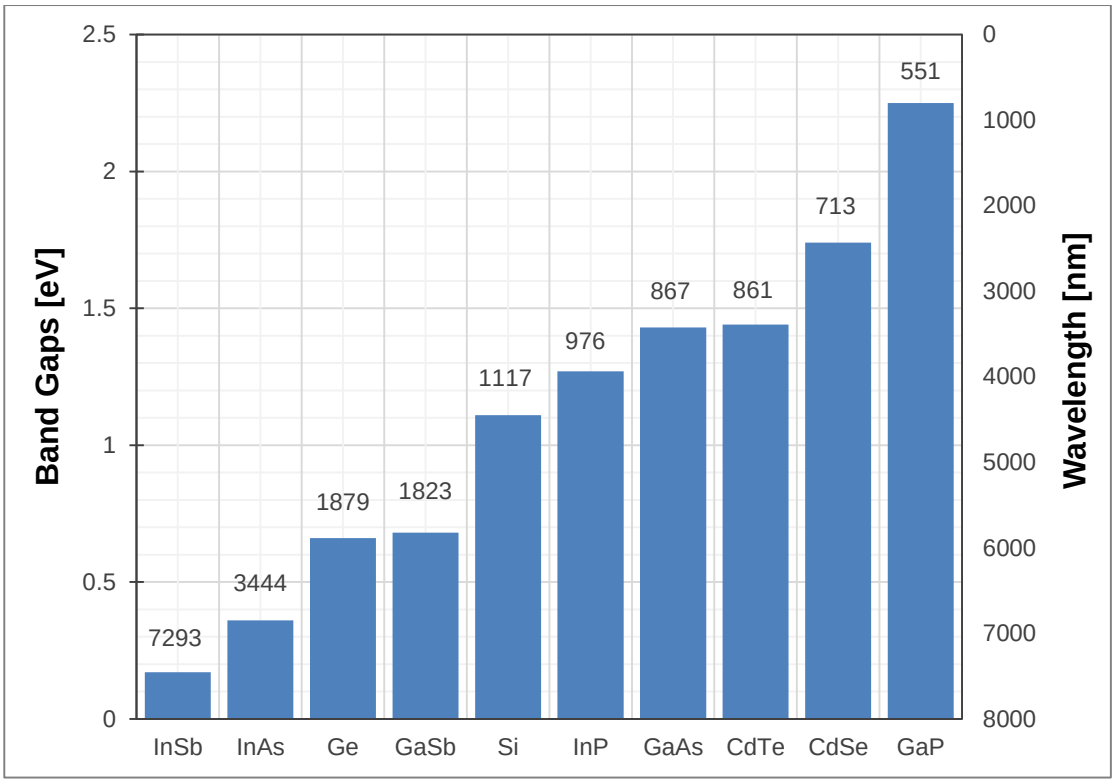

Figure 4. Band gap levels of typical semiconducting materials and corresponding light's wavelength values. Data gathered from Georgia State University [5] and Michigan State University [6].

Among the materials mentioned in figure 4, the most popular type of PV material is silicon (Si), due to its photovoltaic characteristic and availability. Silicon material is chemically purified from silica sand into the form of crystalline silicon (c-Si), either monocrystalline or polycrystalline. Production of c-Si solar cells was mainly based on the behaviour of silicone p-n junction mentioned above. Technology for producing crystalline silicon cells is moderately cheap for mass production, so they are the most used materials. Solar cells made from c-Si materials have average efficiency of 15% to 20%, which means that they can convert about 15% to 20% of received sunlight energy. Up to date, more modern technologies have been developed to produce better PV materials, such as thin-film solar cells, or concentrator photovoltaic, which cost more but has better characteristic and their efficiency can reach 20% to 25%. [1, 12]

Typical silicon PV cells are manufactured in the size of 10 cm x 10 cm, which can supply power output between 1 W and 1.5 W at a voltage of 0.5 to 0.6 V, which is not practical for any applications. That's why multiple solar cells are usually connected in series to provide higher voltages, in a PV solar module. [7, 86; 8, 52.] The size of a solar module is designed by manufacturers according to the application's specification. Solar module is the main component of PV generator, which is the heart of every single solar PV system.

2.2 Solar Photovoltaic System Structure

The PV generator is the essential component in a PV system, but it needs to affiliate with many other ones to provide a total solution that functions properly and reliably. A PV system consists of a number of different components and subsystems, which are carefully designed and all-together connected to provide the desired power production. Figure 5 illustrates the typically-found components in a PV system.

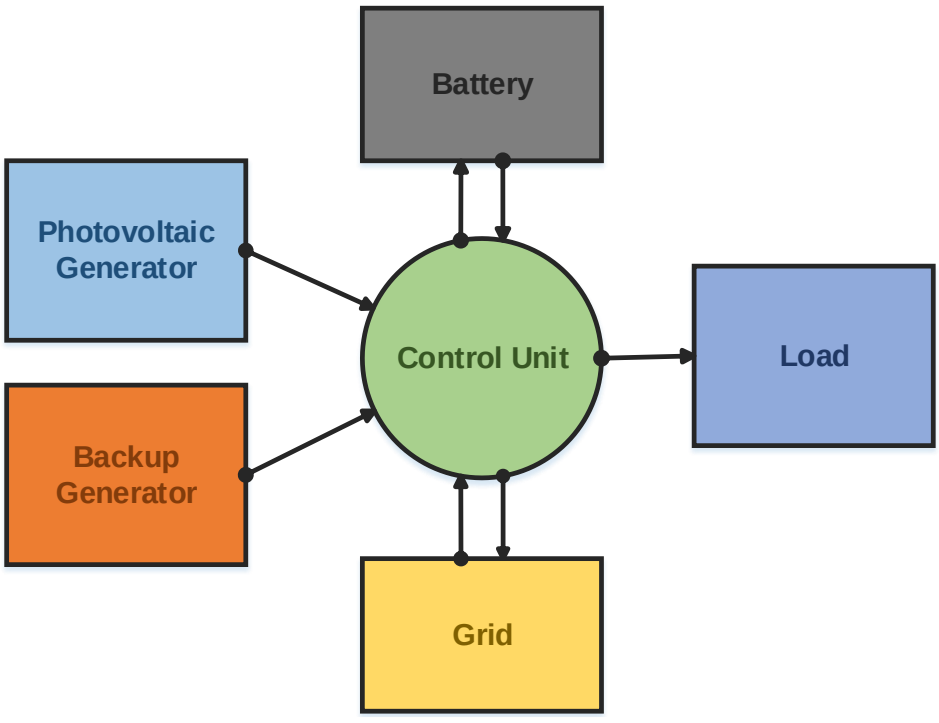

Figure 5. Typical components/subsystems of a solar PV system. Modified from Markvart [7, 84].

The PV generator is the main part or a PV system. It is constructed by connecting multiple PV modules into solar panels, which can be further interconnected to create solar

array for larger power output. The generator is supported by the mechanical module, in either fixed position or tracking rotation. PV generator converts sunlight energy into DC power output which can be utilised in various ways, depending on the application. In small PV systems, DC output is usually consumed by a direct load or charged into a battery for extended use. For even heavier applications, larger PV systems also consist of inverters to provide one-phase or three-phase AC output for industrial uses or residential grid systems.

For the reliable operation of PV generator, it is important to protect individual PV cells in shaded condition. Due to the serial connection of the cells, the shaded one may act as a load due to forward bias. Consequently, the current generated from the other cells may heat up the shaded one and burn it up, leading to system failure. This problem is prevented by using *bypass diodes*, to provide an alternative path for the PV current if some cell is shaded. [8, 52-53] Additionally, in applications that use PV generator to charge a battery, a *blocking diode* is used to prevent PV cells from loading the battery when they are inactive (shaded condition).

Energy converted from the sunlight varies the whole time, so storing that energy is usually a requirement. Chemical battery is a popular choice for energy storage. To charge the battery, PV systems use charge regulator for the best performance and battery protection. Solar panel protection, charge regulation, light tracking module and other regulating modules are all managed and controlled by the control unit, to ensure the proper functionalities of the system.

All the components or subsystems in a PV system are supported and physically connected by different mechanical components. They are specifically designed to meet the requirements of the application and in adaptation to the working environment. Particular mechanical system, like tracking system, can highly affect the efficiency and performance of the system, as it can influence how well PV generator can absorb sunlight energy. The following section will discuss in more details about the importance of such mechanical module to the performance of solar panels.

2.3 Solar Module's Performance and Solar Tracking System

2.3.1 Solar Panel's Performance by Fixed Mounting

For PV modules that collect solar energy on the Earth's surface level, the incoming solar radiation consists of three main components:

- Direct beam that reaches straight to the Earth's surface without scattering
- Diffuse radiation that scatters when passing through the atmosphere of the Earth
- Albedo radiation that reflect from the Earth's surface

Of the first two components, direct beam holds about 80% to 90% of the solar energy in ideal condition (clear sky). [9, 12; 7, 8] It is the major source of energy for the operation of PV generator. For maximum collection of solar energy, solar panels need to maintain alignment with the Sun's direct beams as long as possible. This concept is quantitatively explained by measuring the incident angle between the direct beams and the panels *i*. For the same amount of incoming direct beams, the effective area of solar panel that collects this radiation is proportional to the cosine of *i*. As a result, the power *P* collected by solar panels can be calculated using equation 1:

$$\mathrm{P} = \mathrm{Pmax} * \cos(\mathrm{i}), \tag{1}$$

where *Pmax* is the maximum power collected when solar panel is correctly aligned. From equation (1) we can calculate the loss of power *a*:

$$\mathrm{a} = \frac{\mathrm{Pmax} - \mathrm{Pmax} * \cos(\mathrm{i})}{\mathrm{Pmax}} = 1 - \cos(\mathrm{i}). \tag{2}$$

.

Equation (2) tells that the more misaligned angle is; the more sunlight energy is lost. This connection is illustrated in figure 6.

Figure 6. Connection between solar panel misalignment and direct power loss.

The graph shown in figure 6 provides an illustrative evaluation of how misalignment affects the output power of PV modules. It is easy to observe that the output power drops almost 15% when solar module misaligns 30 degrees from the Sun. The power drops even faster when the misalign angle increases furthermore. By some calculation using solar radiation data from online database, we can evaluate the output power of a fixed-mount solar system at some location on the Earth surface. For instance, solar radiation data for Helsinki on the date of May 1st 2016 provides sunrise at 05:20, sunset at 21:20 and solar noon at 13:20 [10]. Using these values, we can estimate power output of solar modules for the given time and location, assuming the sky is clear throughout the day. By approximating solar direct beams angle at different time of the day, and calculating power output with equation 1, we can plot a graph that compares calculated power values with the maximum power throughout the day, as shown in figure 7 below. It is noticeable that the output power is above 85% only between 11:00 and 16:00, which means the fixed mount panels are efficient in merely 5 hours. For a typical summer day in Helsinki with more than 10 hours of sunlight in average, a PV system operating with this efficiency is certainly not a good solution to gather solar energy.

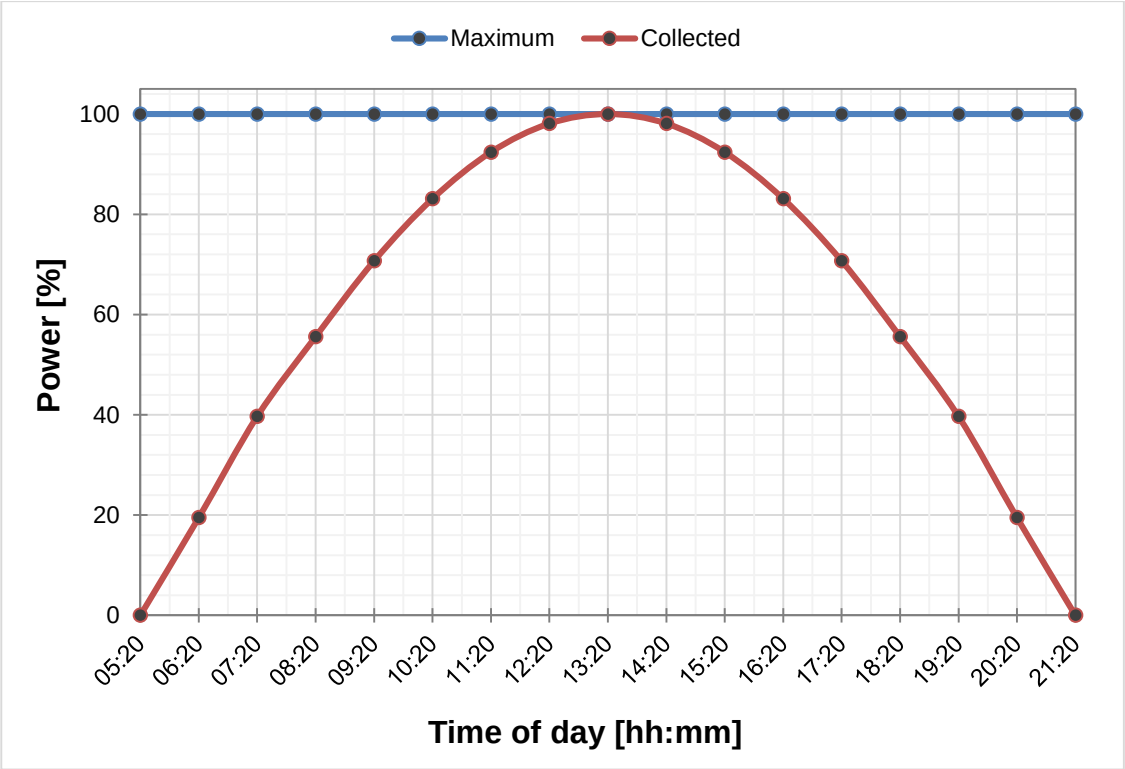

Figure 7. Approximation of power output (red line) compared to maximum output (blue line) for a fix mounted solar module. Data gathered from NOAA Solar Calculator [10].

The calculation explained in figure 7 is only based on an assumption, and doesn't reflect the whole picture. However, it is apparently pointed out that fixed-mount solar panel is not a solution for maximum efficiency, even in ideal weather condition. In reality, there are much more factors that lessen the production of a PV system (cloud shade, seasonal angle change and limited duration of daylight…). In spite of its mechanical simplicity and stability, fixed mount cannot exploit the most of solar panels' capability, therefore not suitable for higher-capacity and more important projects. There is a need of better solutions for mounting the system. We will be subsequently discussing about current solutions of solar tracker for better harvesting of solar power. This subtopic contains useful information for the design and creation of the solar tracking system in this project.

2.3.2 Enhancement by Using Tracking Systems

As discussed above, fix mount options have many drawbacks for the performance of a solar PV system. Solar trackers are able to solve the core problem by minimising the misaligned angle between sunlight's direct beams and the panels. Using different means of mechanical modules, solar trackers can rotate the panels to the optimised position

throughout the whole operation of the system. Comparison of solar trackers' features to fixed mount is explained in table 1.

Table 1. Advantages and disadvantages of trackers over fixed mounts

Advantages	**Disadvantages**
Higher overall efficiency	More complicated design
Higher accuracy	Higher cost
Longer active functioning time	Worse tolerance against weather condition
Better lifetime for solar cells	Consumption of energy (active trackers)
Applicability for different applications	

Solar trackers can use different driving mechanisms to adjust the solar panels' angle, by either passive or active method. Passive trackers operate using two-phase fluid that vaporises and expands when heated by the Sun. The fluid is contained at two sides of passive solar tracker in canisters, connected by a tube. Different expansion due to the Sun's position makes the fluid shifting its weight between two sides of the tracker, cause it to pivot toward the Sun. [11] Passive trackers are less favourable and applicable due to their complex design and low accuracy.

Active trackers on the other hand, utilise motor system to control the movement of panels in single- or dual- axis, by observing the Sun's position using photo sensors. The operation of this type of trackers is managed by controller or computer. Active trackers normally cost more to the system, but provide the best accuracy and efficiency compared to the other solutions. A dual-axis tracker (DAT) can provide additional 40% of solar energy over the year, compared to normal fixed mounting system [7, 92].

2.3.3 Active Solar Trackers

Among the introduced solar tracking systems, active solar tracker is the chosen topic of research for this project, because of its extensive utilisation of electrical and electronic knowledges. It is also the most implemented solution for capturing the sunlight of PV systems. Together with better manufacturing technologies of PV materials, enhancing the operation of active solar trackers is the most efficient way to better exploit the immense energy amount of the Sun.

Based on rotation of solar modules, active solar trackers can be categorised into two main types: single-axis and dual-axis. In single-axis trackers (SAT), solar PV panels are rotated about a single axis that normally aligns with the North meridian. SATs can be configured in a number or ways according to the position of the axis with respect to the ground:

- Tilted single-axis tracker (TSAT)
- Horizontal single-axis tracker (HSAT)
- Vertical single-axis tracker (VSAT).

SATs allow the solar modules to rotate between east-west directions according to the Sun's positions. SATs provide reasonably good balance between flexibility, simplicity and performance. Different configurations of SAT are illustrated in figure 8.

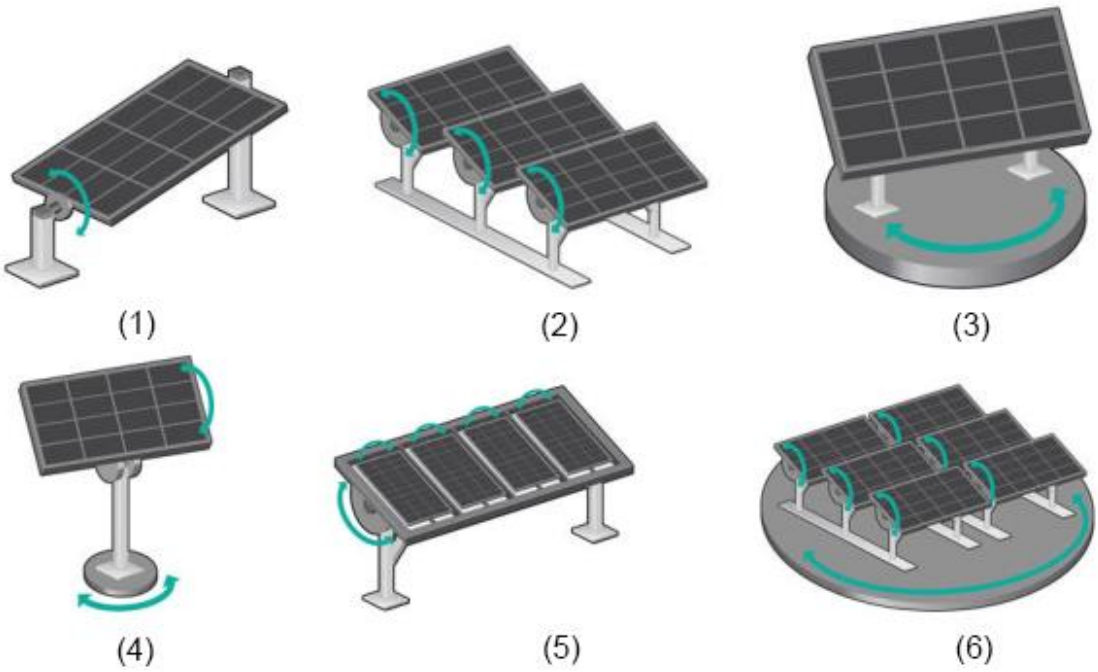

Figure 8. Typical configurations for active solar tracking systems: (1) TSAT (2) HSAT (3) VSAT (4) TTDAT (5) HDAT (6) AADAT. Reprinted from Juda (2013) [12]

Dual-axis tracker (DAT) can be considered the upgrade of SAT, where the freedom of movement is extended to two separate directions. Figure 8 also shows three typical configurations of DAT in the bottom pictures:

- Tip-tilt dual-axis tracker (TTDAT)
- Horizontal dual-axis tracker (HDAT)
- Azimuth-altitude dual-axis tracker (AADAT)

Compared to other types of mounting, DATs allow the widest range of solar modules' movement. Therefore, PV generator will be able to operate at a higher efficiency, for a longer time during sunlight visibility.

It is necessary to clearly understand the term *efficiency* in the context of tracking system enhancement. In this case it means how tracker can make use of PV modules in the best way possible, given that a certain type of PV module is used. Of course DATs cannot increase the "radiation-to-power" efficiency of solar PV materials, but such mounting systems help making the best out of current material technologies. The work of this project will be focusing on implementation of a small-scale TTDAT, based on what have been researched about its structure and operation. The project will be carried out using mainly electronic components and laboratory equipment.

3 Designing of a Solar Tip-tilt Dual-axis Tracker

3.1 Project Planning

3.1.1 Objectives and Scope of the Project

As introduced, the goal of this project was to build a small-scale and functioning TTDAT. Based on the information collected from chapter 2, design of the tracker was created to achieve the following objectives:

- The PV module are firmly mounted on the top of a pole.
- The tracker is able to detect the misalignment between PV module and the Sun's direct beam due to its movement.
- The tracker is able to rotate the PV module in two axes.
- The tracker is able to perform detection and correction repetitively throughout the day.
- Design of the tracker is capable of integrating into bigger systems.
- It's possible to collect output data from the system, for testing and evaluating processes.

Within the scope of a laboratory prototype, design and implementation of this project were not expected to be a complete product for commercial use. They were preferably carried out as a base solution for future development of various applications.

3.1.2 Project Workflow

This project was planned and carried out with the use of Boehm-Spiral methodology. The main approach used to achieve the goal of this project was based on the iterations of work cycles, as being shown in table 2. For the development of the solar tracker, each cycle started by defining existing flaws and necessary improvements of the system. With this new conditions, risk analysis and prototyping were accordingly done. Due to this approach, hardware design and functionality programming of the solar tracker might be altered in each version, to adapt with new objectives.

At the end of each cycle, an enhanced version of the system was expected to be created, with additional functions and better performance. The process underwent with further cycles until the goal of the project was achieved. Boehm-Spiral methodology was applied throughout the project, including both hardware and software designs.

Table 2. Boehm-Spiral methodology stages. Reprinted from Burback (1998) [13].

Cycle	**Step**
Cycle 1 – Early Analysis	Step 1: Objectives, Alternatives, and Constraints Step 2: Risk Analysis and Prototype Step 3: Concept of Operation Step 4: Requirement and Life Cycle Plan Step 5: Objectives, Alternatives, and Constraints Step 6: Risk Analysis and Prototype
Cycle 2 – Final Analysis	Step 7: Simulation, Models, and Benchmarks Step 8: Software Requirements and Validation Step 9: Development Plan Step 10: Objectives, Alternatives, and Constraints Step 11: Risk Analysis and Prototype
Cycle 3 – Design	Step 12: Simulation, Models, and Benchmarks Step 13: Software Product Design, Validation, and Verification Step 14: Integration and Test Plan Step 15: Objectives, Alternatives, and Constraints Step 16: Risk Analysis and Operational Prototype
Cycle 4 – Implementation and Testing	Step 17: Simulation, Models, and Benchmarks Step 18: Detailed Design Step 19: Code Step 20: Unit, Integration, and Acceptance Testing Step 21: Implementation (Deployment)

The methodology explained in table 2 was applied to both hardware and software implementation of the project. The implementation began with aiming to create the most basic and simple features for the device. After they had been all verified, the implementation was recycled again to enhance current features and add new features. This included adjustment or addition of hardware, and modification of the program code. The recycling was repeated until the goals of the project were sufficed. Detailed information of this workflow will be covered in the next sections of this document.

3.2 Hardware Design for a TTDAT System

3.2.1 Selection of Key Components

The first step in building the solar tracker for this project was to set up the necessary hardware. A typical TTDAT system consists of the following units:

- Mounting unit
- Solar panel unit
- Motor unit
- Photo sensor unit
- Microcontroller unit
- Power supply unit
- Other supporting and interconnecting mechanisms.

Design and specification of each unit vary, depending on the application, but their functions and interconnections are almost equivalent. The key components and their functions for designed system of this project are listed in table 3 below.

Table 3. List of main components required for a TTDAT system.

Name of component	**Quantity**	**Functionality**
Polar mount base	1	Holding and connecting all units
Solar module	2	Photovoltaic generators
Solar panel mount	1	Connect solar panel unit to motor unit
Stepper motor	2	Source of rotation
Motor shaft coupler	2	Transmitting motor torque to axes
Motor driver	2	Controlling motor’s rotation
Photoresistor	4	Light sensors for the system
Microcontroller	1	Central intelligence unit of the system
Power supply unit	1	Power input for system’s operation

The configuration of a solar tracker is mainly characterised by the way components are mounted and the placement of stepper motors. For a TTDAT system, photovoltaic module and motor unit are mounted on the top of a pole base. An unused table lamp base was perfectly fit for the size of this project’s device. For source of rotation, two AEG

SO21/24 mini-stepper motors were used, which I had used to handle in a recent project. Image and technical data of the motors are shown in figure 9.

Operating Voltage	**approx. 5 V/0.625 A**
Dimension without axis	**Φ approx. 35 x 25 mm**
Axis	**Φ approx. 1 x 10 mm**
Steps per rotation	**approx. 24**
Motor type	**Bipolar**
Connector	**4**
Resistance per winding	**approx. 8Ω**

Figure 9. AEG SO21/24 mini-stepper motor with technical specifications. Modified from Kemo Electronic GmbH (2009) [14]

For microcontroller to control the rotation of stepper motors, two L293D drivers from Texas Instruments were used. They are a reliable choice for electronic projects that need to drive DC motors. Another important component for motor unit was the shaft coupler, which helped transmitting motor's rotating motion to other components. It was difficult to find small couplers that fit the axis of selected stepper motors (1 mm), so the choice was settled down with generic 5 x 5 mm shaft couplers from the market, which were the smallest available.

Although solar PV panel is the core of a PV system, it was yet to be the major component in the system. The focus of this project, which was a solar tracking system, was rather a subsystem for supporting a complete PV system. Throughout the whole operation of the tracker, the tracking algorithm was totally based on the lighting source, independent from the operation of solar modules. In this design, a small PV panel was integrated into the system, solely for the purpose of testing and evaluating. The PV panel consists of two 90 mm x 60 mm PV modules, which have rated power of 0.6 W at voltage 6 V. Implementation of PV modules requires additional diodes to protect them from loading.

All the parts of the tracker were powered by a breadboard power supply from YwRobot Corporation, as shown in figure 10. It was convenient and practical to supply power to

the system through this supply, as it provided both 3.3 V and 5 V output. The power supply board can be powered using an AC adapter or USB power source.

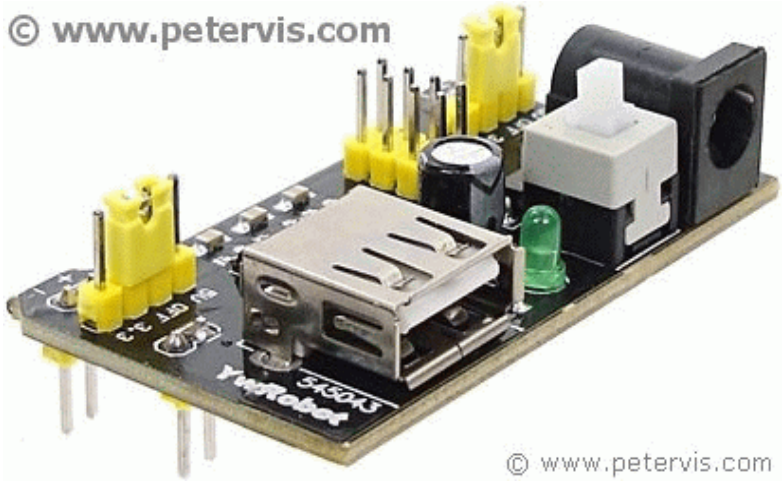

Figure 10. YwRobot Breadboard Power Supply. Reprinted from Vis [15]

As mentioned above, the algorithm for tracking function was based on the lighting source, and for reading the light, four photo sensors were mounted next to PV modules. Photo sensors used in this project were photoresistors, which had resistance depending on light intensity. Signals from those photo sensors were fed into microcontroller as analogue inputs. From the light intensity of all four sensors, the microcontroller was able to determine the incident angle between incoming sunlight and PV modules.

The most important component for the TTDAT system of this project was the microcontroller. It was the brain of the whole system, which managed and controlled all the activity of other parts. Solar tracker in this project utilised mbed NXP LPC1768 microcontroller board from mbed, based on 32-bit ARM Cortex-M3 microprocessor. It was a fast prototyping development board using C/C++ programming language. More on its developing environment are covered on section 3.3.

Beside all the components mentioned above, the work of this project could not be done without other necessary laboratory equipment and materials. Testing and evaluating activities also required certain testing equipment from the laboratory. The implementation of system's hardware will be explained in more details in the next chapter.

3.2.2 Hardware Structure of TTDAT

The block diagram from figure 11 describes the hardware structure of TTDAT system. The most noticeable feature that can be seen from the block diagram is the setup of stepper motors. Stepper motor 1 was mounted directly to the pole of the base, so that its axis aligned with the pole, namely primary axis. To enable the rotation in secondary axis, stepper motor 2 was mounted on top of the first motor, so that two motors were normal to each other. This upright placement of motor helped maintain system balance and reduce unwanted vibration caused by motors' operation.

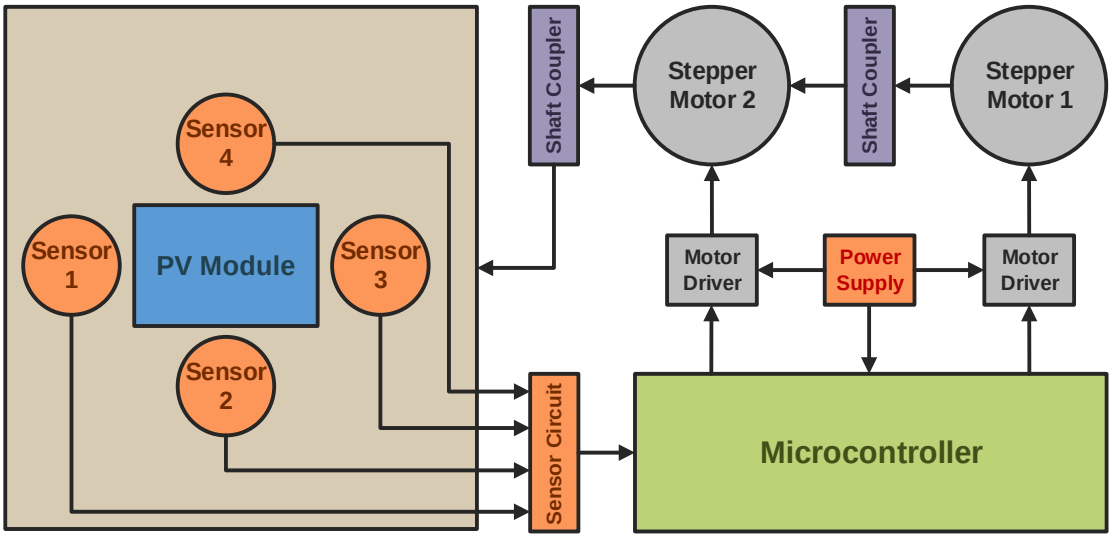

Figure 11. Block diagram for the hardware design

It was impossible to interconnect stepper motors and to connect them to other units without the help of several motor shaft couplers. While primary motor needed to be firmly attached to the pole, PV panel and secondary motor collected its rotating motion through a vertical shaft coupler. The rotation of PV panel in another axis was transmitted from secondary stepper motor through its two horizontal shaft couplers. This way of configuration created a T-shape mechanism that allowed rotating PV panel for almost 180 degrees in east-west and north-south directions (the obstruction of stepper motors' wires were counted in). Figure 12 shows the detailed configuration of rotating mechanism for the TTDAT of this project.

Four photo sensors were installed on the same mount base with photovoltaic modules, so that light rays from the sun came to the sensors and photovoltaic modules with the same angle and intensity. As a result, PV modules could produce its maximum amount

of solar energy when sensory inputs were correctly handled by the microcontroller program. As shown in figure 11, photo sensors were numbered from 1 to 4, and divided into two pairs. Sensor 1 and sensor 3 were at opposite ends, and so were sensor 2 and sensor 4. This placement allowed the device to determine the precise angle between PV modules and incoming sun rays. Photo sensors and PV modules needed to be connected with other electrical components (resistors, protecting diodes…) to be fully functional. These circuits were assembled underneath the mount base for connecting to microcontroller.

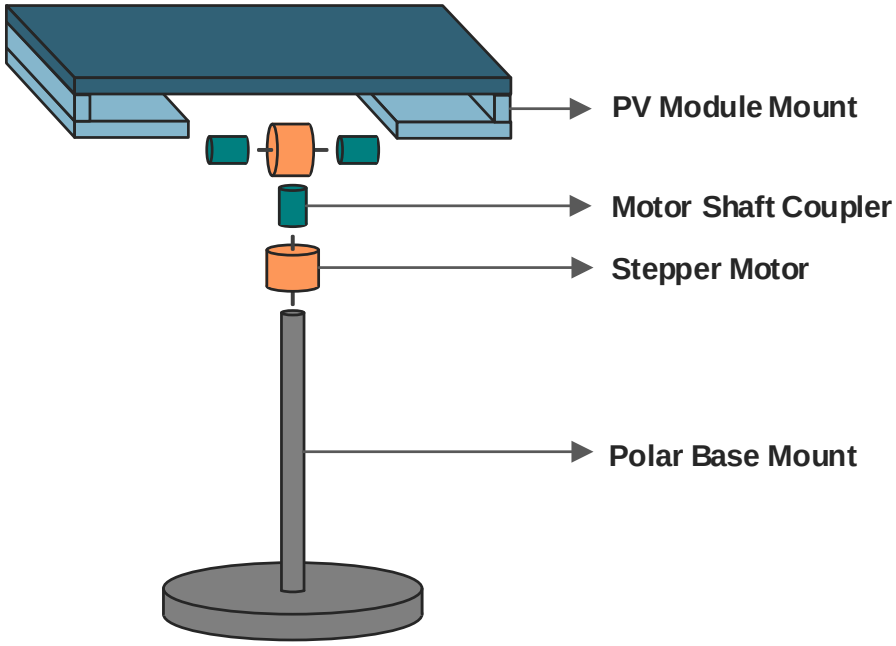

Figure 12. Configuration for mounting stepper motors and PV modules onto pole base.

Finally, microcontroller development board, power supply board, and other associated components were installed on a common prototype board. This board was specifically modified to fit the base of the pole mount. Several designs had been weighed up for the location of this control board, but for the size of device and power of stepper motors, it was settled to be mounted at the lower base for the proper operation of the whole system. Before the actual assembly of motor unit, sensor unit and control board, their functions were carefully tested to ensure that all units worked normally when mounted and connected in the final design. Each single component was also able to be replaced or upgraded when there was a need for that.

With the opted hardware design, the next step of designing the system was carried out. The following section will describe in details the software design for mbed microcontroller of the system.

3.3 Software Design for Tracking Algorithm

As introduced from previous sections, the functions of TTDAT system in this project were programmed in a mbed NXP LPC1768 microcontroller development board. It was a convenient choice for this project, because using the development board is simple and straightforward. Coding for the microcontroller requires basic C/C++ programming language skill, with good support of built-in library and online developer community. Figure 13 shows the mbed microcontroller development board and its pinouts.

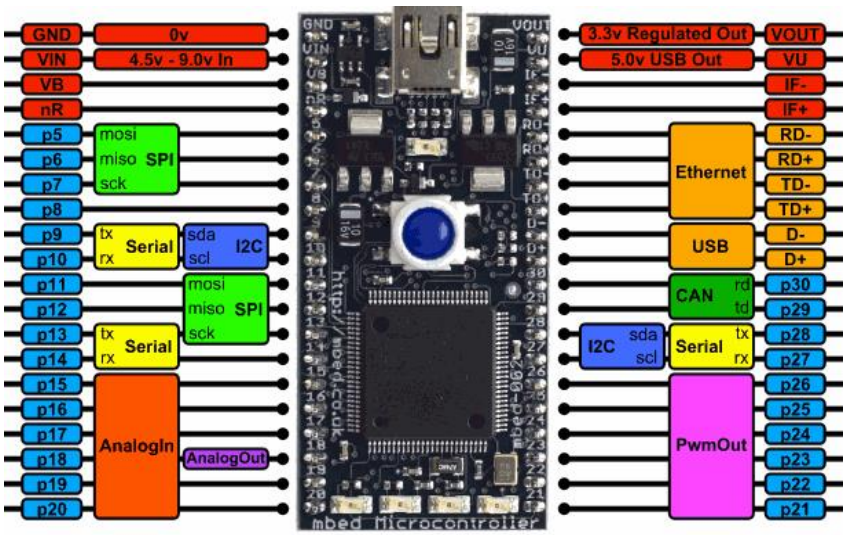

Figure 13. The mbed NXP LPC1768 microcontroller development board with pinout explanation. Reprinted from mbed [16]

The software development kit of mbed controller is fast and lightweight, using an online compiler that requires a user account and registered development board. Compiled programs are downloaded to the computer, and simply copied to the memory of mbed to run it. This helped remarkably accelerating the implementation of software algorithm for this project's device. As shown in figure 13, mbed microcontroller support different interface for various applications. For the solar tracker in this project, analogue input (available from p15 to p20) had been used for reading sensory inputs and other digital output (blue pins) were available for controlling the stepper motor drivers. Built-in power supply

of mbed was also available for sensor circuit, while stepper motor drivers needed to take power separately from the PSU board, as previously shown in figure 11.

For creating a simple and effective algorithm for the program, modularisation was used to determine the logic of the program. Before writing the actual code of the program, it is necessary to define its structure of subdividing modules. Each module handles certain inputs and outputs to provide a specific function. The main loop of the program uses these modules in an appropriate way to provide the desired function of the solar tracker. Figure 14 below shows the modular structure for the algorithm of TTDAT system in this project.

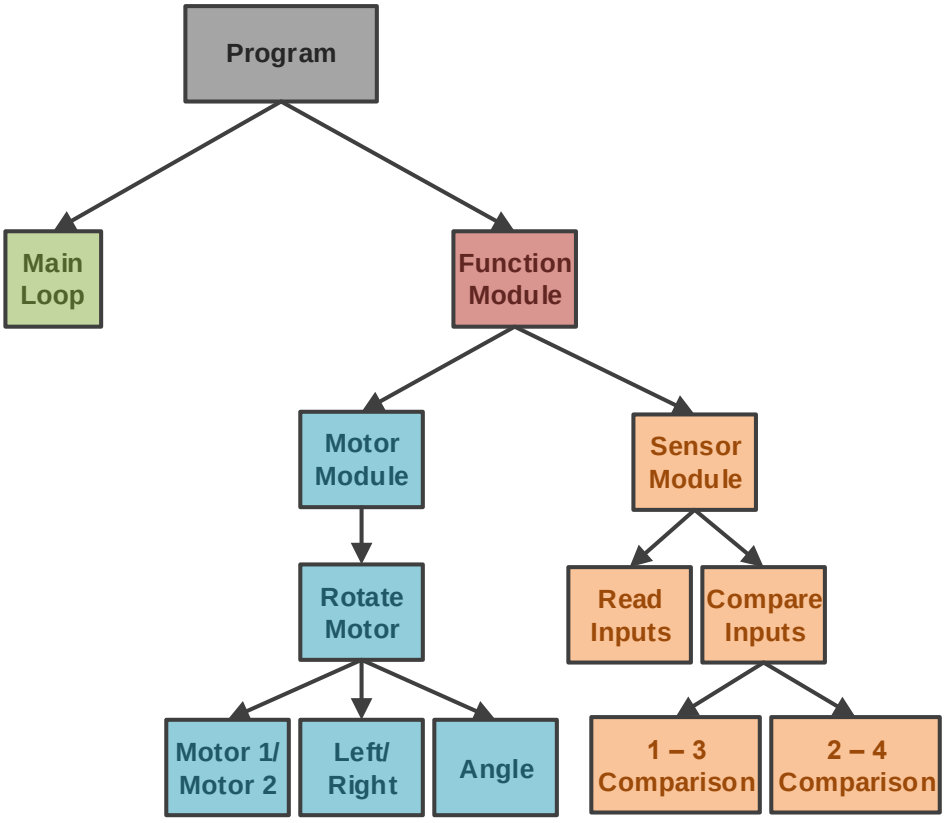

Figure 14. Structure chart showing modular component of solar tracker's program.

From the structure chart, we can see that program of operating TTDAT system consists of two main control modules: motor module, and sensor module. Sensor module receives four inputs from photo sensors through mbed analogue inputs. Its function returns two different outputs: sensor 1 – 3 comparison and sensor 2 – 4 comparison. The function of motor module uses those outputs as parameter to decide the outputs for motor drivers: rotate motor 1 or 2, rotate to the left or right, and the angle of rotation.

Because the operation of the solar tracker is continuous from the moment it is powered on, all the processes of the algorithm must be placed inside an infinite loop, the *main* loop. The main loop contains the sequence of events that happen inside the program from the moment it starts until its state of normal operation. The efficiency of the program depends on how well it makes use of the modules introduced previously. Using the functional modules from figure 14 and the sensor placement from figure 11, the sequence for tracking algorithm main program of the TTDAT system for this project is illustrate in the flow chart below.

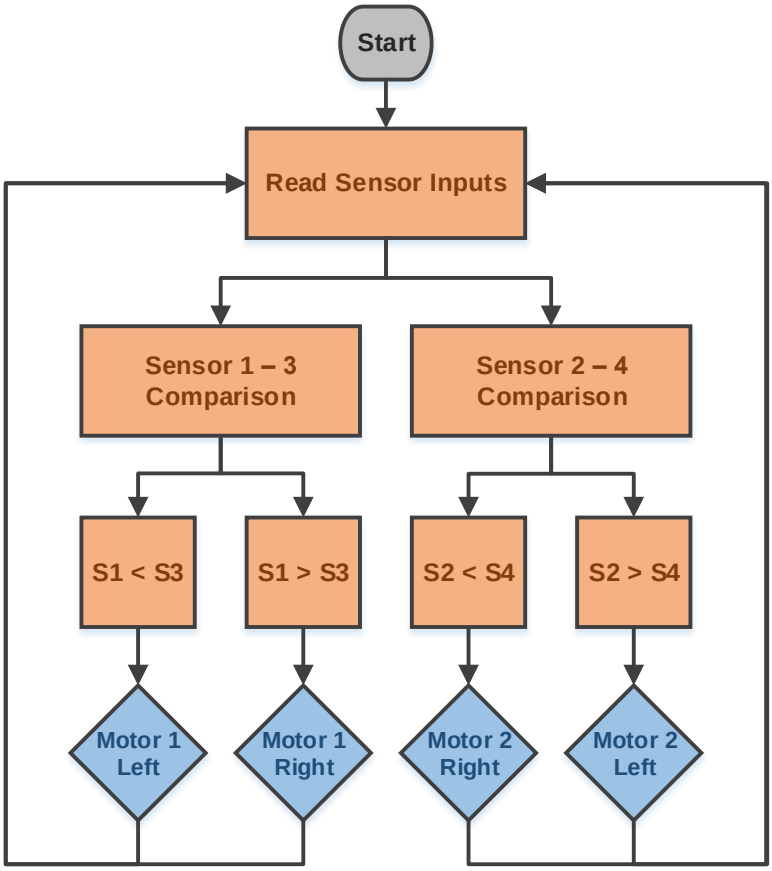

Figure 15. Flowchart of tracking algorithm for TTDAT system.

The information visualised in the structure chart and the flowchart is a useful outline for the actual implementation of the program's code. It helps simplifying the writing of the code, and keeping the workflow on track. Any future update or improvement of the program can be initiated from replotting those charts. In the following chapter, the next stage of the project will be carried out. The chapter contains the information about complete construction of hardware system and creating the code for device's functions.

4 Implementation and Testing of TTDAT

4.1 Hardware Modules Construction

With the completed designing work from previous chapter, the implementation phase of the project was accordingly carried out. This phase began with the construction of hardware for TTDAT system, which included the making of pole mounting base, T-shape mechanism of stepper motors, and mounting plate for photo sensors and PV modules. The stripboard for the control unit was also prepared, ready for final assembling when the microcontroller and motor drivers were programmed and tested.

Figure 16. Final construction of mechanical parts for TTDAT system (top-left: photo sensor/solar module mount, bottom-left: secondary motor, right: polar-mount base with primary motor attached.

Figure 16 shows the main mechanical parts of the TTDAT system, which were built based on the configuration explained in figure 12. The pole-mount base was easily made by removing the upper part of an old table lamp. On the top of the pole, primary stepper motor was attached with the help of plastic harness, and reinforced by duct tape. To form the T-shape transmission mechanism, a shaft coupler was concavely sanded to fit the side of secondary stepper motor, before their joining was firmly held by tape.

As mentioned in section 3.2.1, the smallest shaft couplers that could be found had diameter of 5 mm. To fit those pieces to the stepper motors' shaft, which had diameter of 1 mm, extra intermediate plastic tubes were used to solve this incompatibility. With the help of those extra components, all mechanical parts above could be properly connected, as shown in figure 17. In practical, the T-shape configuration of stepper motor provided maximum rotation range of 360 degrees for primary axis, and 150 degrees for secondary axis. With a beneficial tracking algorithm of microcontroller program, this rotation capability could track the sun at most possible positions during active operation of TTDAT system.

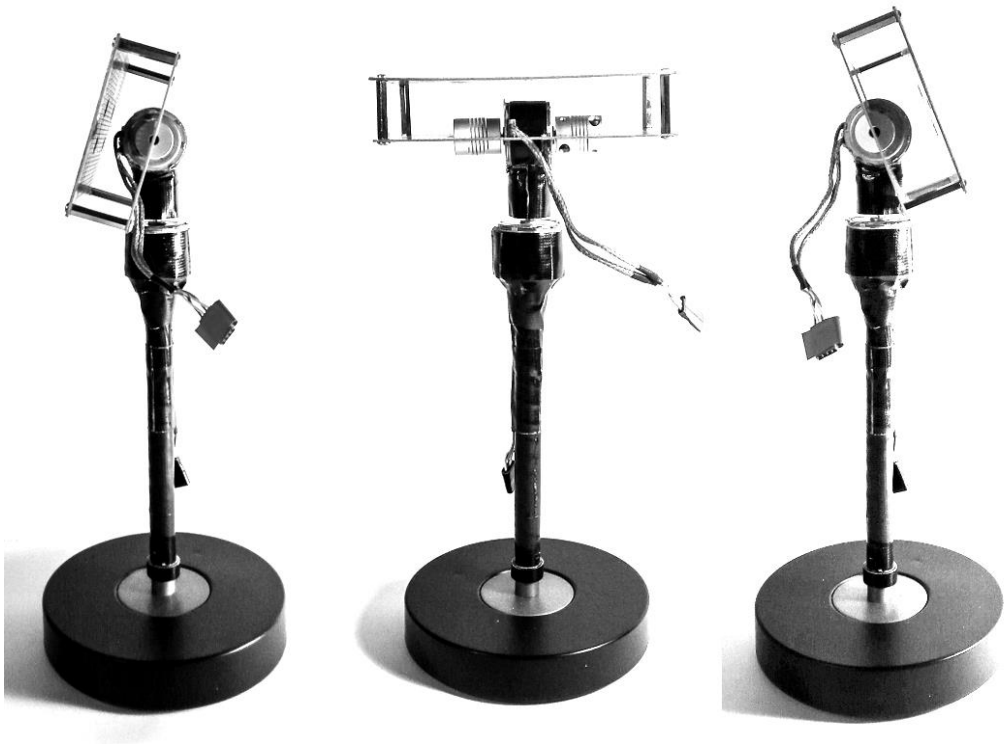

Figure 17. Assembly of TTDAT hardware, with its positions of maximum secondary rotation.

Before the assembling of the control unit, microcontroller and other electrical components was only connected, programmed and tested on a solderless breadboard. They were later arranged and installed on a stripboard using dual in-line package (DIP) connectors. DIPs were chosen for easy installing and configuring the components, as well as future upgrades or adjustments. The arrangement and placement of components on the control board are displayed in figure 18.

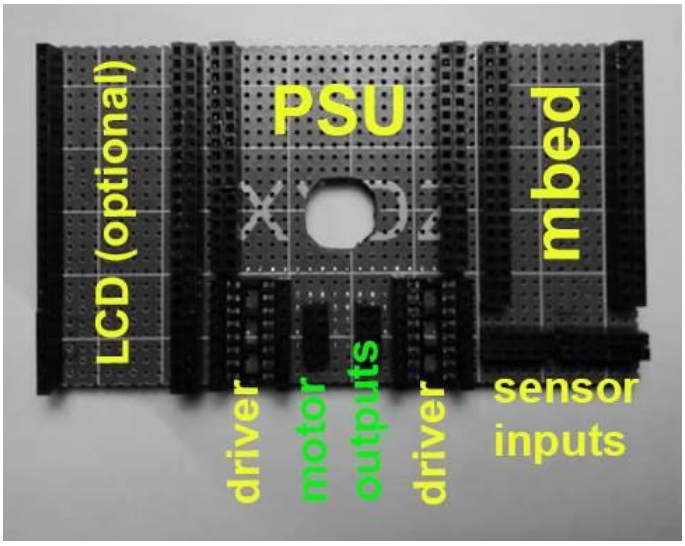

Figure 18. Placement of electrical components on the control board.

The control board was fitted into the base of the device by cutting a hole at the centre, with an insulating layer underneath. This project used jumper cables to connect components on the board, for easy development. Extended cables were also needed to connect the control unit with stepper motors and sensor circuit, due to their distant placement.

Before the development of device's tracking algorithm could be carried out, the circuit for mbed microcontroller and other components needed to be correctly set up. The diagram in figure 19 shows how mbed microcontroller was connected to other components. As introduced from section 3.3, the microcontroller sent outputs to L293D motor drivers through digital output pins. Each driver required one enabling input and four controlling inputs. To connect stepper motors to their drivers, extending cables were used, because they were already mounted to the base of device. The sensor circuit was connected to microcontroller by simply feeding its voltage divider outputs to four analogue inputs of mbed.

All components were operating using power from the PSU unit, including the mbed microcontroller. Additionally, when the development board was connected to a computer, USB power could be conveniently used for testing the functionality of the system.

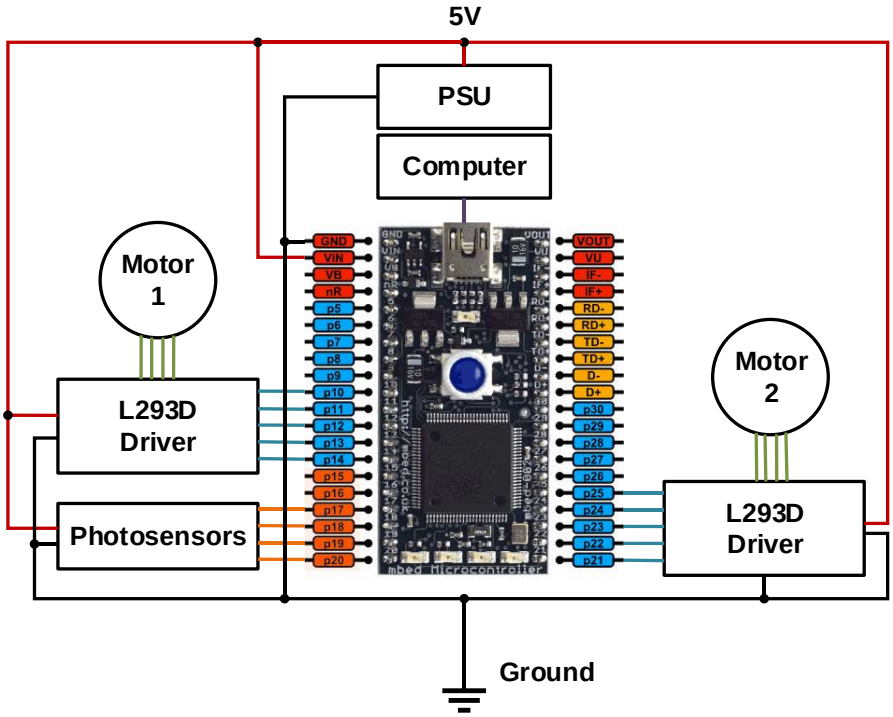

Figure 19. Simplified setup of device's components for tracking algorithm development.

The diagram in figure 19 only describes the overview of controlling circuit. The detailed and comprehensive diagram with correct pinout connections can be found at appendix 1 of this document.

4.2 Software Implementation for Initial Prototype

4.2.1 Functionality Programming

All the coding and compiling for the software of the TTDAT system were completed on the online compiler of mbed website, which can be accessed from the address *https://developer.mbed.org/compiler*. With a developer account, we can carry out the developing work from any web browser, on multiple platforms. Compiled programs were downloaded to the computer, and transferred to mbed internal storage through USB connection. The software implementation of the TTDAT system was done with the guideline of the structure chart and flow chart in figure 14 and figure 15.

The developing work started with building the functional module for stepper motor drivers. A small library for stepper motor drive was created, and can be imported to the main program using the following syntax:

```
#include "StepperMotor.h"
```

Listing 1. C++ syntax for importing stepper motor functional module.

In the initial version, the stepper motor library from listing 1 provides the basic functions for the motor driver, including:

- Initialising instance of *stepper* class for each motor driver and assigning digital output pins from mbed to each one.
- Enabling or disabling any motor.
- Turning motor to the left or right by one step.

A simple *main* program was created to test and adjust the movement of stepper motor. Creating an instance for stepper motor driver is straightforward, by declaring an object of type *stepper*, and specifying its five control outputs from mbed microcontroller. As it has been initialised, it is available to use any function of the *stepper* class that was included in its module code. I decided to add other advanced features only in later versions of the program. At this stage of the implementation, it was only necessary to use the essential feature of motor drivers to test the functionality of stepper motor, and how it performed with the hardware design of the system.

The next step of software implementation was reading the inputs signal from photo sensors. Instead of creating modular library, photo sensor inputs can be easily read by creating four *AnalogIn* variables in the *main* program, which corresponds to the analogue inputs p17 to p20 of mbed, as shown in figure 19. Prior to the coding task of sensor, the photo sensor circuit needed to be correctly configured and installed to the top mount of the device. The photo sensors used in this project are of Light-Dependent Resistor (LDR) type, which have resistance value in outdoor daylight condition of 50 to 60 Ω, and dark condition of more than 1 KΩ. As displayed in figure 20, each LDR was connected in series with a 150 Ω resistor, to form a voltage divider circuit, where resistor voltage outputs *Vout* were fed into analogue inputs of mbed microcontroller. With selected value of components, *Vout* can have voltage values approximately from 0 V to 3.3 V, which are compatible with analogue input voltage of the mbed.

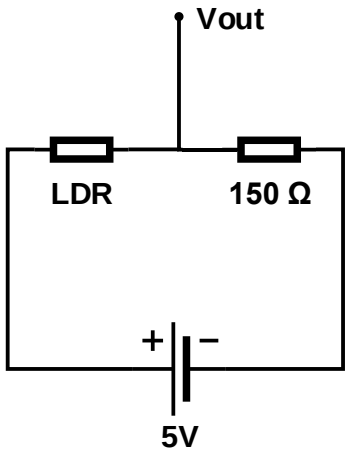

Figure 20. Circuit diagram for photo sensor circuit.

After reading the value of those analogue input, decision for the rotation of stepper motor were made by using *if* statements and appropriate functions from *stepper* module. Detailed coding for decision making was done in accordance with the logic defined in figure 15. By adding different variables for LED indicators into the code, and compiling the program to mbed microcontroller, we can check whether stepper motors can rotate in the expected direction and photo sensors can correctly read light intensity.

4.2.2 Testing of Device Functionality

Because LDR photo sensor can work with any kind of visible light, testing process for the initial prototype was completed indoor using table lamp as source of light. In the first test, the device was able to detect the movement of light source and rotate to align with it. Light detection had some small delay, due to the characteristic of LDR photo sensor, but that is acceptable for solar PV applications, because the sun moves slowly and gradually during device's operation.

Unfortunately, the first version of the TTDAT system did not have enough stability. The weight of all the components mounted on top of secondary stepper motor put a strain on it, which cause improper and incorrect rotation from time to time. Also, in practical, the stepper motors only worked properly with 12 steps per rotation, which resulted in imperfect alignment of photo sensors, causing repetitive realignments. Under the scope of this project, it was hard to circumvent these drawbacks without replacing stepper motors with better ones.

Another noticeable flaw in the software design of the system is the obstruction of secondary motor's cable. As it was mounted on top of primary motor, the whole component, including its cable, rotated when the system detected changes of inputs from sensor 1 and 3. Extensive rotation of primary motor in one direction caused the cable to twist, and finally prevented the operation of the tracker. The *stepper* module of the microcontroller program was yet to be included function to detect and avoid this terminal flaw. This led to some prototype revision of the system, which is discussed in subsequent section. More comprehensive testing and evaluating of TTDAT would be carried out when the whole system has been fully implemented and revised.

4.3 Prototype Revisions

To resolve the problem of motor cable that was mentioned in the previous section, a small enhancement had been applied to the hardware design of TTDAT system. Two extra LDR photo sensors were connected to mbed to help determining current rotation state of primary stepper motor. These additional sensors were attached to the shaft coupler between two motors (moving part), to detect the light from two LEDs attached to primary motor (static part). Alignment of these couples of components generated high output voltages V1 and V2, which were fed into mbed controller as digital inputs. Using these indicators with the modification of program's code, we can prevent the problem discovered in section 4.2.2.

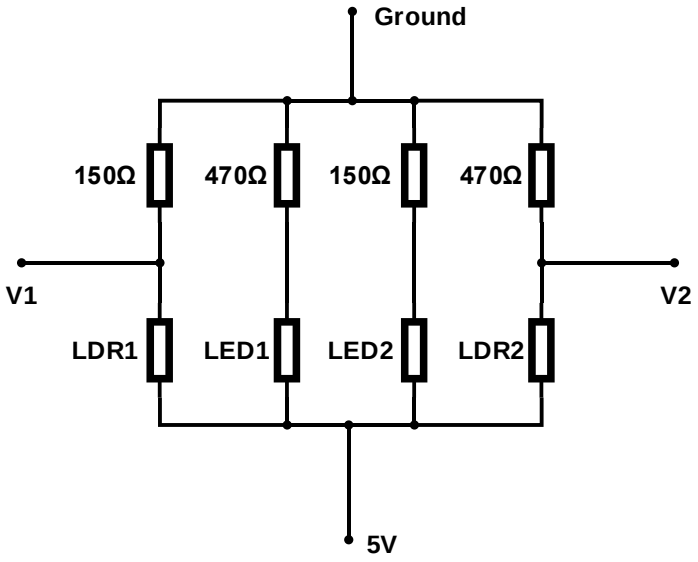

Figure 21. Circuit diagram for additional photosensors.

In reality, the LDR photo sensors and LEDs were not directly connected. Power and signal cables for LEDs were combined with secondary motor's cable to avoid complication. To make use of the added components, the *stepper* module of microprocessor program was modified. Two indicating inputs were included as members of the class, in which their values were used as end-of-range conditions. The algorithm for that logic can be summarised in the following pseudo code:

```
read indicator1; read indicator2;
(end of range) is (rotate disable);
if (rotate left and (indicator is 1)) or (rotate right
and (indicator is 0)) then (end of range is 1);
```

Listing 2. Pseudo code for detecting end of rotation range.

When there is a need to implement more advanced functions, the method explained in listing 2 can be applied to write a calibrating procedure, or reset function for the system.

As the updated version of the code had been confirmed, the program was compiled and transfer to mbed microcontroller. All the components were installed onto the control stripboard, which was afterward mounted to the base of the device. The implementation of the system was finalised by installing PV modules onto the top mount of the device. The TTDAT system was then brought outdoor for evaluating the performance of PV modules.

4.4 Evaluation of TTDAT in Improving PV Panel's Efficiency

The main purpose of this stage was to perform a quantitative evaluation of how much the designed TTDAT improves over normal fixed mount PV systems. In order to do that, an identical solar PV panel was used on a fixed mount at equal height with TTDAT. PV panel of in fixed mount configuration was placed horizontally. The two systems were placed outside, under the same weather condition, with the same setup of measuring equipment, which are shown in figure 22 below.

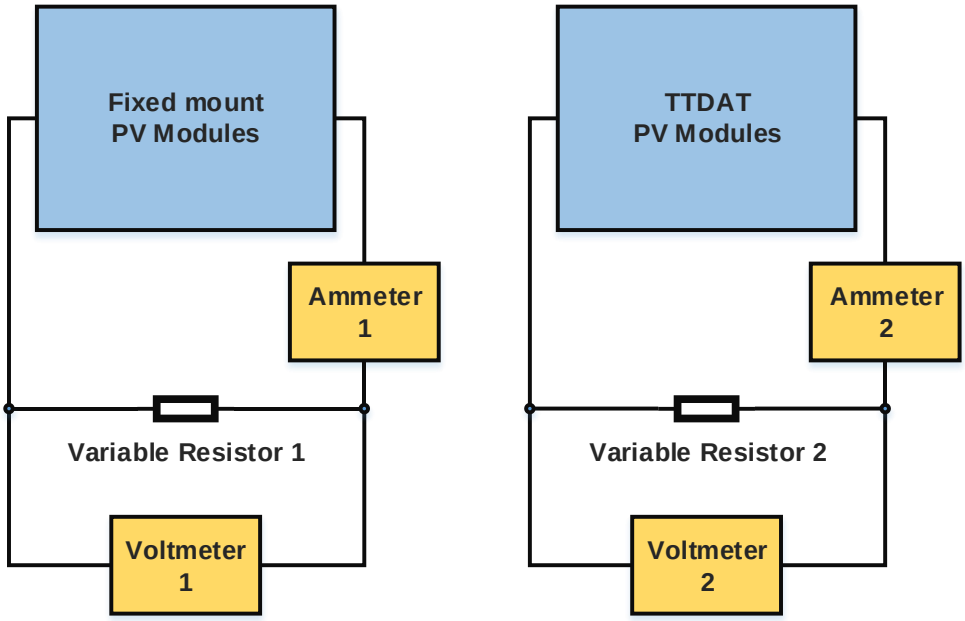

Figure 22. Device setup for measuring PV modules output power.

In each system, the solar PV panel consisted of two PV modules in series connection. Each module had rated power output of 0.6 W at voltage 6 V, giving the total rated output of 1.2 W at voltage 12 V. With the way of set up measuring equipment as in figure 22, the variable resistor provided a more detailed result of performance of two systems with different loads. The evaluation had been carried out on a summer day in May 2016, with the following goals:

- Measurements are done in multiple sessions during different time of the day.
- In each session, it is important that two systems are measured simultaneously, under the same solar radiation.
- Measurements include open-circuit voltage, short-circuit current, output voltage and current at different loads in the range 10 Ω to 10 KΩ.

With the provided goals, six sessions were carried out, where voltage and current values for ten different load value were recorded. After the sessions, all output power values of two systems were calculated using data collected from the measurements. From those data, we can observe how well TTDAT system improves the output of PV modules, compared to fixed mount system. Measured data of open-circuit voltages and short-circuit current of two systems are display in table 4, which was taken from appendix 3.

Table 4. Open-circuit voltages and short-circuit currents of PV modules mounted on two systems.

Time of day	Fixed Mount System		TTDAT System	
	Open-circuit Voltage [V]	Short-circuit Current [mA]	Open-circuit Voltage [V]	Short-circuit Current [mA]
09:30	13.28	61.30	13.52	103.0
11:30	13.60	79.00	13.86	115.0
13:30	13.30	77.00	13.50	102.5
15:30	13.28	58.50	13.60	105.5
17:30	13.01	32.00	13.73	87.60
19.30	12.39	9.400	13.81	46.00

It is unarguable to see how TTDAT system exceled over fixed mount system when the testing time shifted to the end of the day. Output data from both systems were heavily degraded as the Sun moved closer to the horizon, where its radiation got absorbed and diffused by the Earth's atmosphere. However, while fixed mount system was further attenuated due to its misalignment, TTDAT system still managed to convert a considerable amount of solar energy, which was much more impressive. It is also necessary to note that at the location where measurements were taken (northern hemisphere), seasonal inclination of the Earth always causes a *seasonal misalignment* for the horizontal fixed mount. Tracking systems, or course, are not affected by this phenomenon.

5 Results and Discussion

At the end of the project, a small-scale and functional tip-tilt dual axis solar tracker shown in figure 23 has been completely designed and implemented. The final product, in the size of a table lamp, was able to perform the basic functions of a TTDAT system:

- Rotating a PV panel in two different axes
- Detecting the misalignment between PV panel and the sun
- Correctly rotating PV panel to realign PV panel

Figure 23. Final hardware design of TTDAT system.

Under the functionality test, the device was able to detect and follow the movement of an observable light source. This applied for both indoor light (from a floor lamp) and outdoor light (sunlight). The solar tracker made use of the stepper motors properly, which enabled a wide range of rotation for the PV panel as expected. Moreover, extensive measurements of PV modules performance with the help of TTDAT system has proved its noticeable improvement over PV systems with fixed mount. A graph showing this comparison using the data from the test is illustrated in figure 24.

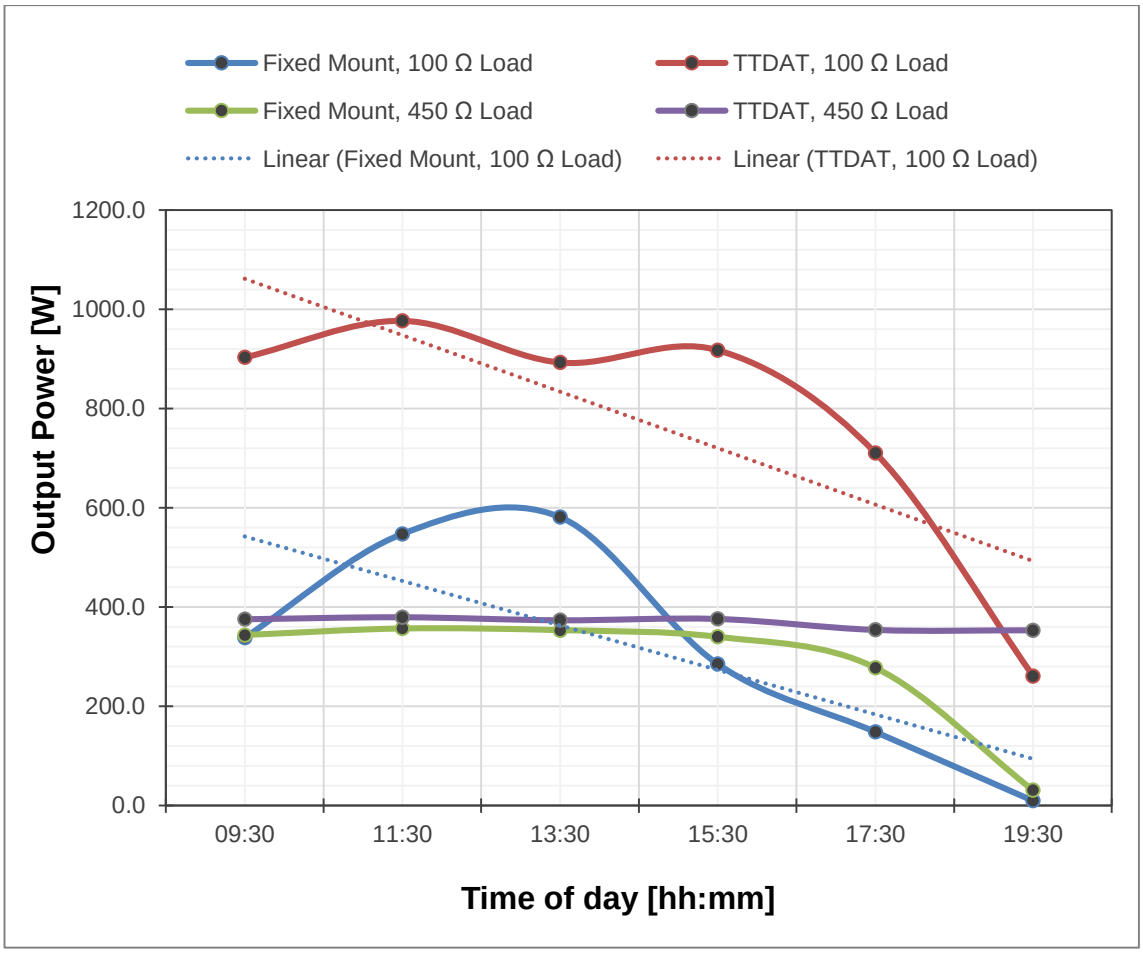

Figure 24. Measured power outputs with 100 Ω and 450 Ω loads.

The sample data shown in figure 24 tell that the improvement of TTDAT system over fixed mount varies as the load value changed. There's no big difference between two systems when driving high load (450 Ω), while for smaller load (100 Ω), the TTDAT power output is almost double of the other one. That's why it is important to consider the application when choosing PV modules for the system.

Overall, it can be concluded that these results have met the initial goals of the project, and the functionality of device has sufficed the design requirements. Also practical performance of the system is in accordance with theoretical background knowledge.

The solar tracker, however, was yet to be a perfect device without drawbacks and limitations. In the first implementation, the obstruction of motor cables was a bothersome shortcoming. Twisting of cables limited the rotation of stepper motors, and prevented the tracker from operation every now and then. This had been resolved in the upgraded

design, with the use of additional measuring hardware and modifications of the micro-controller program. Although absolute resolution for this problem requires rearrangement of stepper motors and the mounting configuration of control board, the approach was not studied in the scope of this project.

The limited utilisation of stepper motors was also a factor that affected the precision of the device. In the manufacturer's specifications, the motors were rated about 24 steps per rotation. However, different programming approaches of controlling the motor drivers had succeeded at only 12 steps per rotation. This resulted in imperfect aligning function of the tracker, where misalignment could be up to 15 degrees or energy loss of 3.4%. The incorrect alignment also activated more frequent realignments, which drew more energy. In actual commercial projects, it is recommended to using high quality motors for better precision.

There was one final limitation in project execution that needed to be mentioned. Testing process for the device and all the collected results were performed on a fine day in summer. It is still unclear about how well the system's functions behave in harsh or unsteady conditions. As a laboratory prototype, this system needs more extensive testing and examination, so that the hardware design and function algorithm can be further improved for practical use.

In general, the project was a successful attempt of researching and applying knowledge of current technology to create a laboratory prototype that can function as other commercial product. For future development, the design of TTDAT system in this project can still be useful to apply into other projects, such as upgraded versions of current system or its design variations for different applications.

6 Conclusion

The goal of the project was to design and implement a small scale prototype of tip-tilt dual-axis solar tracker with basic tracking functions. Designing and implementing processes have been accordingly completed for the work of the project. The final result was a complete design of such a system, with functionality that met the design requirements.

While the project has succeeded in creating a device with basic required features, there are still considerable drawbacks and limitations with the performance of the device, as discussed in the implementation work of the project. It is possible to overcome these limitations and to improve the performance of the device in future development.

The project was a successful effort in fulfilling the purpose when I started it, that is to research and catch up with current technologies in this field of energy exploitation. It is a useful reference for those who needs to develop similar systems. The knowledge and information from this project can also become the starting point for future development of a various of applications.

References

1 International Energy Agency, “Technology Roadmap - Solar Photovoltaic Energy - 2014 Edition,” IEA Publications, 2014.

2 Nipun, "Difference Between p-type and n-type Semiconductor," 19 October 2015. [Online].
URL: http://pediaa.com/difference-between-p-type-and-n-type-semiconductor/.
Accessed 2 May 2016.

3 Wikimedia Foundation, Inc., "Depletion region," Wikimedia Foundation, Inc., 5 May 2016. [Online].
URL: https://en.wikipedia.org/wiki/Depletion_region.
Accessed 27 May 2016.

4 Apec Virtual Center, Japan, "Principle of Electricity Generation by Photovoltaic Cells," 2007. [Online].
URL: http://www.apec-vc.or.jp/e/modules/tinyd00/index.php?id=74.
Accessed 10 May 2016.

5 R. Nave, "Semiconductor Band Gaps," [Online].
URL: http://hyperphysics.phy-astr.gsu.edu/hbase/tables/semgap.html.
Accessed 20 April 2016.

6 Michigan State University | Department of Chemistry, "Frequency - Wavelength - Energy Converter," [Online].
URL: https://www2.chemistry.msu.edu/faculty/reusch/virttxtjml/cnvcalc.htm.
Accessed 14 May 2016.

7 T. Markvart, Ed., Solar Electricity, 2nd ed., Chichester, West Sussex: Wiley, 2000.

8 R. Messenger and A. Abtahi, Photovoltaic Systems Engineering, 3rd ed., CRC Press, 2010.

9 B. Marion, C. Riordan and D. Renné, “Shining On,” Solar Radiation Resource Assessment Project, May 1992. [Online].
URL: http://www.nrel.gov/docs/legosti/old/4856.pdf.
Accessed 26 April 2016.

10 Earth System Research Laboratory, "NOAA Solar Calculator," [Online].
URL: http://www.esrl.noaa.gov/gmd/grad/solcalc/.
Accessed 20 May 2016.

11 N. J. Parmar, A. N. Parmar and V. S. Gautam, “Passive Solar Tracking System,” International Journal of Emerging Technology and Advanced Engineering, vol. 5, no. 1, January 2015.

12 C. Juda, "5 Ways to Track Your Solar Tracker," 18 January 2013. [Online].
URL: http://blog.pepperl-fuchs.us/blog/bid/253098/5-Ways-to-Track-Your-Solar-Tracker.
Accessed 20 April 2016.

13 R. L. Burback, "Software Engineering Methodology: The WaterSluice," 14 December 1998. [Online].
URL: http://infolab.stanford.edu/~burback/watersluice/node299.html.
Accessed 15 May 2016.

14 Kemo Electronic GmbH, “P5337 Mini-stepper motor "AEG SO21/24",” 16 September 2009. [Online].
URL: https://www.kemo-electronic.de/en/Components/Elements/Motor/P5337-Mini-stepper-motor-AEG-SO21-24.php.
Accessed 1 May 2016.

15 P. J. Vis, “YwRobot Breadboard Power Supply,” [Online].
URL: http://www.petervis.com/Raspberry_PI/Breadboard_Power_Supply/YwRobot_Breadboard_Power_Supply.html.
Accessed 15 May 2016.

16 mbed, "mbed LPC1768," mbed, [Online].
URL: https://developer.mbed.org/platforms/mbed-LPC1768/.
Accessed 10 May 2016.

Circuit Diagram for TTDAT Control Board and Photo Sensor Circuit

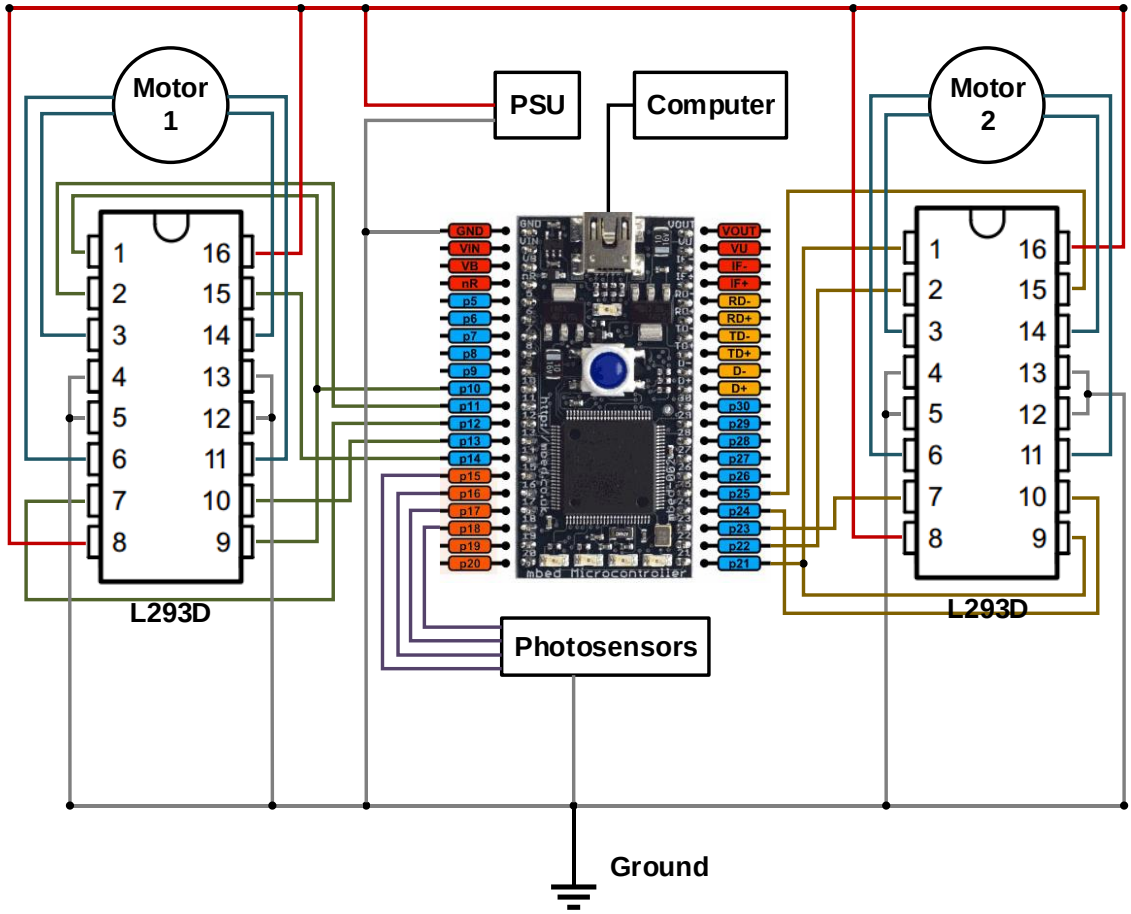

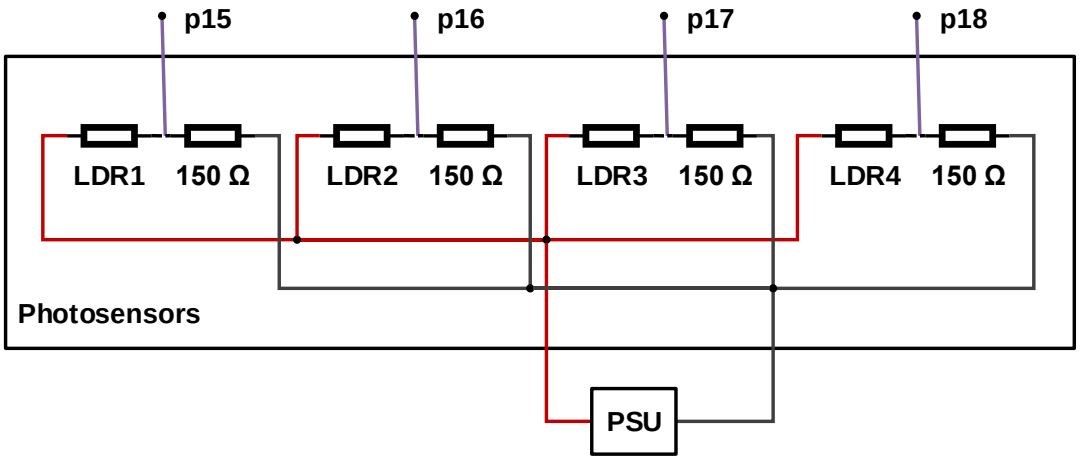

Stepper Motor Functional Module and TTDAT Software Program Code

Filename: StepperMotor.h

```
#ifndef STEPPER_MOTOR_H
#define STEPPER_MOTOR_H
#include "mbed.h"

/* A StepperMotor interface for driving 4-wired stepper motors
 * using L293D driver
 *
 * @code
 * #include "mbed.h"
 * #include "StepperMotor.h"
 * Stepper motor1(p5, p6, p7, p8, p9, p10, p11); // en, a1-a4,
 * i1-2
 * int main() {
 *     motor1.enable();
 *     motor1.left();
 *     motor1.disable();
 * }
 * @endcode
 */

class Stepper {
public:
    /* Create a Motor interface
     * @param en              Enable
     * @param a1-a4           Control outputs
     * @param i1-i2           End-of-range Input Indicator
     */
    Stepper(PinName en, PinName a1, PinName a2, PinName a3,
    PinName a4, PinName i1, PinName i2);

    /* Function prototypes */

    // Turn motor to the left
    void left(void);

    // Turn motor to the right
    void right(void);

    // Enable motor
    void enable(void);

    // Disable motor
    void disable(void);

private:
    DigitalOut _en, _a1, _a2, _a3, _a4, _i1, _i2;
};
#endif
```

Filename: StepperMotor.cpp

```
#include "StepperMotor.h"

Stepper::Stepper(PinName en, PinName a1, PinName a2, PinName a3,
                 PinName a4, PinName i1, PinName i2) :
                 _en(en), _a1(a1), _a2(a2), _a3(a3), _a4(a4),
                 _i1(i1), _i2(i2){

    // Default values
    _en = 0;
    _a1 = 0;
    _a2 = 0;
    _a3 = 0;
    _a4 = 0;
    _i1 = 0;
    _i2 = 0;
}

// Rotate to the right
void Stepper::right() {

    _a3 = _a4 = 0;

    if(_a1) {
        _a1 = 0; _a2 = 1;
        wait(0.1);
    }
    else if(_a2) {
        _a1 = 1; _a2 = 0;
        wait(0.1);
    }
    else {
        _a1 = 1; _a2 = 1;
        wait(0.1);
        _a1 = 0; _a2 = 1;
        wait(0.1);
        _a1 = 1; _a2 = 0;
        wait(0.1);
    }
}

// Rotate to the left
void Stepper::left() {

    _a1 = _a2 = 0;

    if(_a3) {
        _a3 = 0; _a4 = 1;
        wait(0.1);
    }
    else if(_a4) {
```

```
            _a3 = 1; _a4 = 0;
            wait(0.1);
        }
        else {
            _a3 = 1; _a4 = 1;
            wait(0.1);
            _a3 = 0; _a4 = 1;
            wait(0.1);
            _a3 = 1; _a4 = 0;
            wait(0.1);
        }
}

void Stepper::enable() {
    _en = 1;
}

void Stepper::disable() {
    _en = 0;
}
```

Filename: main.cpp

```
#include "mbed.h"
#include "StepperMotor.h"

Stepper motor1(p10, p11, p12, p13, p14, p8, p9);
Stepper motor2(p21, p22, p23, p24, p25, p26, p27);
AnalogIn s1(p17), s2(p18), s3(p19), s4(p20);

int main() {
    while(1) {
        // enable motor 1 when s1 and s3 are not balanced
        if (s1 != s3){
            motor1.enable();
        }
        else {
            motor1.disable();
        }

        // enable motor 2 when s2 and s4 are not balanced
        if (s2 != s4){
            motor2.enable();
        }
        else {
            motor2.disable();
        }

        // rotate motor according to sensor input
        while (s1 < s3){
            motor1.left();
        }
        while (s1 > s3){
            motor1.right();
        }
        while (s2 < s4){
            motor2.right();
```

```
            }
            while (s2 > s4){
                motor2.left();
            }
        }
    }
```

Measurement Data of Fixed Mount System and TTDAT System

Time of day	Fixed Mount System		TTDAT System	
	Open-circuit Voltage [V]	Short-circuit Current [mA]	Open-circuit Voltage [V]	Short-circuit Current [mA]
09:30	13.28	61.30	13.52	103.0
11:30	13.60	79.00	13.86	115.0
13:30	13.30	77.00	13.50	102.5
15:30	13.28	58.50	13.60	105.5
17:30	13.01	32.00	13.73	87.60
19:30	12.39	9.400	13.81	46.00

R = 10Ω	Fixed Mount System			TTDAT System		
Time of day	Voltage [V]	Current [mA]	Calculated Power [mW]	Voltage [V]	Current [mA]	Calculated Power [mW]
09:30	0.610	73.50	44.84	0.950	99.80	94.81
11:30	0.670	72.20	48.37	1.030	112.5	115.9
13:30	0.720	78.70	56.66	0.910	100.9	91.82
15:30	0.540	71.50	38.61	1.000	102.8	102.8
17:30	0.650	36.70	23.86	1.360	84.80	115.3
19:30	0.080	9.270	0.742	0.530	52.20	27.67

R = 47Ω	Fixed Mount System			TTDAT System		
Time of day	Voltage [V]	Current [mA]	Calculated Power [mW]	Voltage [V]	Current [mA]	Calculated Power [mW]
09:30	2.710	58.90	159.6	4.870	102.4	498.7
11:30	3.530	75.00	264.8	5.300	109.2	578.8
13:30	3.520	75.60	266.1	4.670	100.0	467.0
15:30	2.560	54.60	139.8	4.910	104.7	514.1
17:30	1.910	37.70	72.00	4.060	84.90	344.7
19:30	0.460	10.27	4.724	2.440	51.00	124.4

R = 100Ω	Fixed Mount System			TTDAT System		
Time of day	Voltage [V]	Current [mA]	Calculated Power [mW]	Voltage [V]	Current [mA]	Calculated Power [mW]
09:30	6.120	55.30	338.4	9.610	94.00	903.3
11:30	7.300	75.00	547.5	10.04	97.30	976.9
13:30	7.750	75.00	581.3	9.560	93.40	892.9
15:30	5.320	53.60	285.2	9.660	95.00	917.7
17:30	4.110	36.10	148.4	8.500	83.60	710.6
19:30	0.990	9.660	9.563	5.090	51.30	261.1

R = 200Ω	Fixed Mount System			TTDAT System		
Time of day	Voltage [V]	Current [mA]	Calculated Power [mW]	Voltage [V]	Current [mA]	Calculated Power [mW]
09:30	10.12	53.20	538.4	11.78	67.10	790.4
11:30	11.17	60.00	670.2	11.95	64.20	767.2
13:30	11.25	60.60	681.8	11.93	64.50	769.5
15:30	9.710	51.90	503.9	11.77	67.50	794.5
17:30	7.400	36.10	267.1	11.63	64.50	750.1
19:30	1.740	8.800	15.31	8.000	44.60	356.8

R = 450Ω	Fixed Mount System			TTDAT System		
Time of day	Voltage [V]	Current [mA]	Calculated Power [mW]	Voltage [V]	Current [mA]	Calculated Power [mW]
09:30	12.18	28.20	343.5	12.82	29.30	375.6
11:30	12.60	28.30	356.6	13.00	29.20	379.6
13:30	12.53	28.20	353.3	12.88	29.00	373.5
15:30	12.18	27.90	339.8	12.84	29.30	376.2
17:30	11.66	23.80	277.5	13.11	27.00	354.0
19:30	3.690	8.410	31.03	12.44	28.40	353.3

R = 1KΩ	Fixed Mount System			TTDAT System		
Time of day	Voltage [V]	Current [mA]	Calculated Power [mW]	Voltage [V]	Current [mA]	Calculated Power [mW]
09:30	12.82	12.70	162.8	13.25	13.10	173.6
11:30	12.86	12.61	162.2	13.16	12.93	170.2
13:30	12.97	12.80	166.0	13.22	13.10	173.2
15:30	12.75	12.55	160.0	13.27	13.00	172.5
17:30	12.59	12.24	154.1	13.50	13.26	179.0
19:30	8.210	8.180	67.16	13.23	12.76	168.8

R = 2KΩ	Fixed Mount System			TTDAT System		
Time of day	Voltage [V]	Current [mA]	Calculated Power [mW]	Voltage [V]	Current [mA]	Calculated Power [mW]
09:30	13.04	6.310	82.28	13.32	6.470	86.18
11:30	13.00	6.310	82.03	13.30	6.450	85.79
13:30	13.19	6.350	83.76	13.45	6.470	87.02
15:30	12.82	6.290	80.64	13.27	6.490	86.12
17:30	12.83	6.360	81.60	13.62	6.820	92.89
19:30	10.73	5.200	55.80	13.38	6.490	86.84

R = 4KΩ	Fixed Mount System			TTDAT System		
Time of day	Voltage [V]	Current [mA]	Calculated Power [mW]	Voltage [V]	Current [mA]	Calculated Power [mW]
09:30	13.00	3.260	42.38	13.35	3.360	44.86
11:30	13.16	3.240	42.64	13.45	3.310	44.52
13:30	13.24	3.240	42.90	13.47	3.300	44.45
15:30	12.85	3.280	42.15	13.30	3.400	45.22
17:30	12.98	3.19	41.41	13.76	3.400	46.78
19:30	11.26	2.760	31.08	13.41	3.300	44.25

R = 7.5KΩ	Fixed Mount System			TTDAT System		
Time of day	Voltage [V]	Current [mA]	Calculated Power [mW]	Voltage [V]	Current [mA]	Calculated Power [mW]
09:30	13.10	1.710	22.40	13.45	1.730	23.27
11:30	13.23	1.730	22.89	13.49	1.760	23.74
13:30	13.27	1.730	22.96	13.50	1.760	23.76
15:30	12.95	1.680	21.76	13.39	1.740	23.30
17:30	12.92	1.680	21.71	13.80	1.790	24.70
19:30	11.58	1.520	17.60	13.49	1.770	23.88

R = 9.8KΩ	Fixed Mount System			TTDAT System		
Time of day	Voltage [V]	Current [mA]	Calculated Power [mW]	Voltage [V]	Current [mA]	Calculated Power [mW]
09:30	13.05	1.310	17.10	13.50	1.350	18.23
11:30	13.30	1.330	17.69	13.54	1.350	18.28
13:30	13.29	1.320	17.54	13.50	1.380	18.63
15:30	13.00	1.300	16.90	13.44	1.340	18.01
17:30	12.97	1.290	16.73	13.81	1.380	19.06
19:30	11.78	1.140	13.43	13.47	1.330	17.92